ANALYSIS
https://doi.org/10.1038/s41893-020-00646-7

nature sustainability

Economic footprint of California wildfires in 2018

Daoping Wang[1,9], Dabo Guan[2,3,9] ✉, Shupeng Zhu[4], Michael Mac Kinnon[4], Guannan Geng[5], Qiang Zhang[2], Heran Zheng[6], Tianyang Lei[2], Shuai Shao[7], Peng Gong[2] and Steven J. Davis[8]

Recent increases in the frequency and scale of wildfires worldwide have raised concerns about the influence of climate change and associated socioeconomic costs. In the western United States, the hazard of wildfire has been increasing for decades. Here, we use a combination of physical, epidemiological and economic models to estimate the economic impacts of California wildfires in 2018, including the value of destroyed and damaged capital, the health costs related to air pollution exposure and indirect losses due to broader economic disruption cascading along with regional and national supply chains. Our estimation shows that wildfire damages in 2018 totalled $148.5 (126.1–192.9) billion (roughly 1.5% of California's annual gross domestic product), with $27.7 billion (19%) in capital losses, $32.2 billion (22%) in health costs and $88.6 billion (59%) in indirect losses (all values in US$). Our results reveal that the majority of economic impacts related to California wildfires may be indirect and often affect industry sectors and locations distant from the fires (for example, 52% of the indirect losses—31% of total losses—in 2018 were outside of California). Our findings and methods provide new information for decision makers tasked with protecting lives and key production sectors and reducing the economic damages of future wildfires.

The frequency and size of wildfires in the western United States has been increasing for several decades, driven by climate-change-related decreases in precipitation and related changes in the moisture in vegetation[1–5]. Meanwhile, land and fire management have probably exacerbated the hazard[6], and population and economic growth—especially at the wildland–urban interface[7]—has dramatically increased the human exposure to fires. The combined result has been ever rising wildfire risks, culminating in California in a series of enormously damaging fires in 2017, 2018 and 2020. To date, efforts to quantify the impacts of specific fires on humans (for example, by researchers, but also by insurance companies, public agencies and the media) have focused on the physical and direct damage to infrastructure and loss of life[8]. The potential human health effects of wildfire smoke are also increasingly recognized, but only rarely estimated[9,10]. But disasters may also have large indirect impacts on economic activities that extend much beyond the location of physical destruction or smoke[11–13]. For example, destruction of productive capital and interruption of transportation systems or labour supply affect other economic activities up and down all connected supply chains. Such economic disruption by fires has never been quantified; our understanding of the magnitude of wildfire impacts and their distribution across space and industries may thus be incomplete. In turn, decision makers (including government officials, businesses and residents) may systematically underestimate wildfire risks and thereby misallocate resources intended to recover from past fires and/or build up resilience to future ones.

In this article, we use a combination of approaches to evaluate the full economic footprint of California wildfires that occurred in 2018. These fires were the deadliest and among the most destructive of any year in California history up to that time: 8,527 fires burned an area of 1.9 million acres (7,700 km^2; approaching 2% of the state's area)[14]. Table 1 lists the 17 largest fires by area burned, along with their location in the state and duration. Details of our analytical approach and data sources are provided in the Methods. In summary, we estimate capital losses as the costs to repair and rebuild damaged or destroyed assets based on data from the US National Interagency Fire Center's Large Incident Year-to-Date Report[14] and valuations compiled from insurance companies (for example, Munich RE[15]). We then estimate morbidity, mortality and health cost (for example, medical expenses, lost working time and so on) related to fire-related air pollution using the most up-to-date emissions inventory from the fourth-generation global fire emissions database (GFED4)[16], a regional chemical transport model (based on the state-of-the-science model GEOS-Chem), and the US Environmental Protection Agency's Benefits Mapping and Analysis Program (BenMAP)[17]. Finally, we estimate indirect losses of economic disruption to 80 industry sectors in each of California's 58 counties and the rest of the United States using the multiregional disaster footprint (MRDF) model[18–20] (Methods).

Results

Figure 1 shows modelled results of monthly average particulate matter ≤2.5 μm ($PM_{2.5}$) concentrations related to California wildfires between July and December of 2018 along with the corresponding areas of California with unhealthy air quality. Major fires in July occurred in both the northern parts of the state (for example, the Pawnee, Klamathon, Carr, Mendocino Complex and Whaleback fires; Table 1 and Supplementary Fig. 1) and the Sierra Nevada (for example, the Lions and Ferguson fires) (Fig. 1a). Altogether, fires destroyed 472 structures in July and negatively affected air quality throughout much of the northern half of the state, especially in Shasta, Glenn and Tehama counties in the north and Mariposa, Tuolumne and Madera counties in the Sierra Nevada (Table 1 and Fig. 1a). At the worst, on 30 July, the air quality of over 39 million acres was categorized as unhealthy or worse—roughly 31% of the

[1]School of Urban and Regional Science, Shanghai University of Finance and Economics, Shanghai, China. [2]Department of Earth System Science, Tsinghua University, Beijing, China. [3]The Bartlett School of Construction and Project Management, University College London, London, UK. [4]Advanced Power and Energy Program, University of California, Irvine, Irvine, CA, USA. [5]State Key Joint Laboratory of Environmental Simulation and Pollution Control, School of Environment, Tsinghua University, Beijing, China. [6]Industrial Ecology Programme, Norwegian University of Science and Technology, Trondheim, Norway. [7]School of Business, East China University of Science and Technology, Shanghai, China. [8]Department of Earth System Science, University of California, Irvine, Irvine, CA, USA. [9]These authors contributed equally: Daoping Wang, Dabo Guan. ✉e-mail: guandabo@tsinghua.edu.cn

Table 1 | Seventeen largest fires by area burned in California in 2018

Name	Cause	Start date	End date	County	Size (acres)	Suppression cost (in million US$)	Structures destroyed
Pawnee	Human	23 June	7 July	Lake	15,185	36.5	22
Lions	Lightning	23 June	6 September	Madera	12,990	13.9	0
Waverly	Unclear	29 June	2 July	San Joaquin	11,789	2.5	3
County	Human	30 June	13 July	Yolo	90,288	46.9	30
Klamathon	Unclear	5 July	21 July	Siskiyou	38,008	33.5	82
Ferguson	Unclear	14 July	23 August	Mariposa	96,901	118.5	11
Carr	Human	23 July	29 August	Shasta	229,651	158.8	1,604
Cranston	Human	25 July	8 August	Riverside	13,139	22.1	12
Whaleback	Unclear	27 July	6 August	Lassen	18,703	8.9	0
Mendocino Complex	Unclear	28 July	17 September	Colusa, Glenn, Lake, Mendocino	459,123	201.0	280
Donnell	Unclear	2 August	6 September	Tuolumne	36,450	33.6	135
Holy	Unclear	6 August	3 September	Orange, Riverside	23,025	25.70	24
Hirz	Human	9 August	13 September	Shasta	46,150	55.5	0
Stone	Lightning	15 August	29 August	Modoc	39,387	16.9	2
Delta	Human	5 September	6 October	Shasta	63,311	64.4	45
Camp	Unclear	8 November	25 November	Butte	153,336	102.8	18,804
Woolsey	Unclear	8 November	20 November	Los Angeles, Ventura	96,949	56.9	1,643

Data from the US National Large Incident Year-to-Date Report 2018[14].

state's area; 31% of the state's population lives in these areas. Many of the fires that began in July or even June of 2018 were still burning and spreading in August, when still more fires started in both the north (for example, the Hirz and Stone fires; Table 1) and the Sierra Nevada (for example, the Donnell fire), as well as in the southern parts of the state (for example, the Holy fire; Fig. 1b). The fires destroyed an additional 1,618 structures in August and further degraded air quality over an even larger area: as of 5 August, air quality of 36 million acres was categorized as unhealthy or worse (29% of the state's area; 25% of the state's population lives in these areas; Fig. 1b). All the major fires begun before September ended in early September due to increases of precipitation, and the Delta fire in Shasta County was the only new major fire that began in September (on the 5th). As a result, fire-related air pollution was much lower in September; at the worst, unhealthy air spanned 6.95 million acres in the northernmost part of the state on 7 September (5.6% of the state's population lives in these areas; Fig. 1c). The Delta fire destroyed 45 structures and was not fully contained until 6 October. The break in major fires continued throughout October, such that fire-related air pollution remained low (Fig. 1d). On 8 November, we saw the start of the last two major fires of the year, the Camp in Northern California and the Woolsey in Southern California, which contributed to the destruction of 20,447 structures in November. These fires also substantially degraded air quality throughout the northern Central Valley, Bay Area and north coast counties; on 17 November, air quality was categorized as unhealthy or worse over 18.61 million acres (39.0% of the state's population lives in these areas; Fig. 1e).

Figure 2 shows our estimates of fire-related damages from the 2018 fires in total and broken down by capital losses, health costs and indirect losses of economic disruption (mean results of the sensitivity analysis; see Supplementary Table 1 for county-level damages in each category). Of $27.7 billion in capital losses, $4.5 billion (17%) belonged to households and $23.2 billion (83%) were productive capital, that is, commercial, industrial or public assets. The greatest capital losses of any individual fire were those related to the Camp fire in Butte County, which totalled $14.6 billion (53% of all capital losses; Supplementary Fig. 2). This helps to explain the disproportionately large capital losses in the northern parts of the state, with Ventura and Los Angeles counties showing up as southern hotspots of capital losses (Fig. 2a). Given the larger populations of these southern counties, per capita capital losses were not as great, however (Fig. 2b). Health costs fall into three categories: mortality, medical expenses and work time lost. Mortality dominates the total. We estimate 3,652 air pollution deaths were caused by California's 2018 fires, which—applying the value of statistical life—represent a loss of $32.2 billion. Note that the deaths related to air pollution are considerably greater than the reported 104 lives (including 98 civilians and 6 firefighters) that were claimed directly by the fires. In comparison to the deaths, the costs related to medical expenses and work time lost are relatively small: $210 million and $130 million, respectively. The geographical distribution of the health costs reflects a combination of the areas most affected by wildfire-related $PM_{2.5}$ (Fig. 1) and populated areas. Thus, overall health costs in the Bay Area and Sacramento–San Joaquin Delta and Los Angeles metropolitan area are particularly large—despite the fact that some of the affected counties had no major fires (Fig. 2c and Table 1). By contrast, per capita health costs more closely reflect the highest concentrations of wildfire-related $PM_{2.5}$ (Figs. 1 and 2d).

Our estimates of indirect losses caused by fire-related economic disruptions in 2018 are considerably larger than either direct capital losses or health costs. Total losses in the United States were $88.6 billion—more than 0.4% of the nation's gross domestic product (GDP) that year. Of this total, $42.7 billion (48.2%) of the indirect losses occurred in California, and $45.9 billion (51.8%) occurred in other parts of the United States via production and consumption supply chains connected to California. Despite having no major fires itself, Sacramento County suffered the greatest indirect losses, $6.6 billion (8% of the county's GDP that year; Supplementary Table 1). However, as a share of GDP, Butte County (where the Camp fire occurred in November) suffered even greater indirect losses: $5.6 billion, or 47.4% of its own GDP. Combining the damages in all

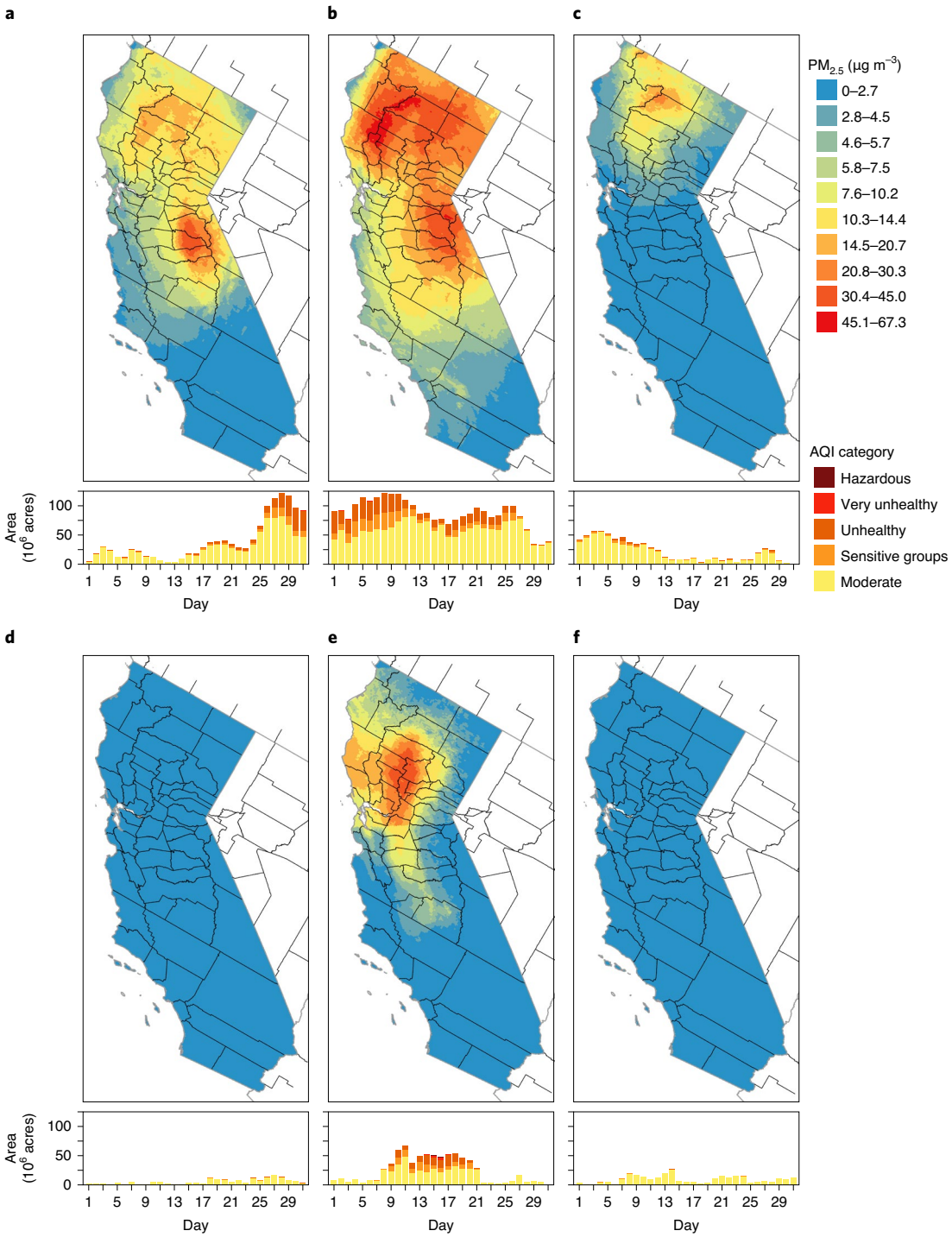

Fig. 1 | Air pollution due to fire emissions from July to December in California. a–f, Monthly mean $PM_{2.5}$ concentrations induced by fire emissions (map at the top of each panel) and the area in each air quality index (AQI) category in California (bar chart at the bottom of each panel; refer to Mintz[51] for the criteria) for July (**a**), August (**b**), September (**c**), October (**d**), November (**e**) and December (**f**); data for county boundary lines from the Geography Program of the United States Census Bureau (www.census.gov/programs-surveys/geography.html). In the maps, pollutant concentrations from low to high are indicated using shades from cool colour to warm colour (blue–yellow–red). In the bar charts, the area statistics in each air quality category are shown in stacked bar charts (some grids on simulated boundaries, outside California, are counted). Wildfires in July, August, September and November release large amounts of pollutants into the air (maps; **a**,**b**,**c**,**e**): from July to September, wildfires in Northern California (for example, the Carr fire in Shasta County from 23 July to 29 August; the Mendocino complex fire in Colusa, Glenn, Lake, and Mendocino counties from 28 July to 17 September; Table 1 and Supplementary Fig. 1) and the Sierra Nevada (for example, the Ferguson fire in Mariposa County from 14 July to 23 August; the Lions fire in Madera County from 23 June to 6 September) caused monthly concentrations of local air pollutants to increase by more than 10 $\mu g\,m^{-3}$ (up to about 60 $\mu g\,m^{-3}$) (maps; **a**–**c**); In November, the Camp fire in Butte County (Northern California) considerably increased the concentration of pollutants in the air (**e**). Fire pollutants can spread over great distances, resulting in poor air quality in unburned areas (bars; **a**,**b**,**c**,**e**): from late July to early September and mid-November, air quality in many areas of California was not in the 'good' category (0–15.4 $\mu g\,m^{-3}$). Note that the area in the bar charts includes the boundary the model area.

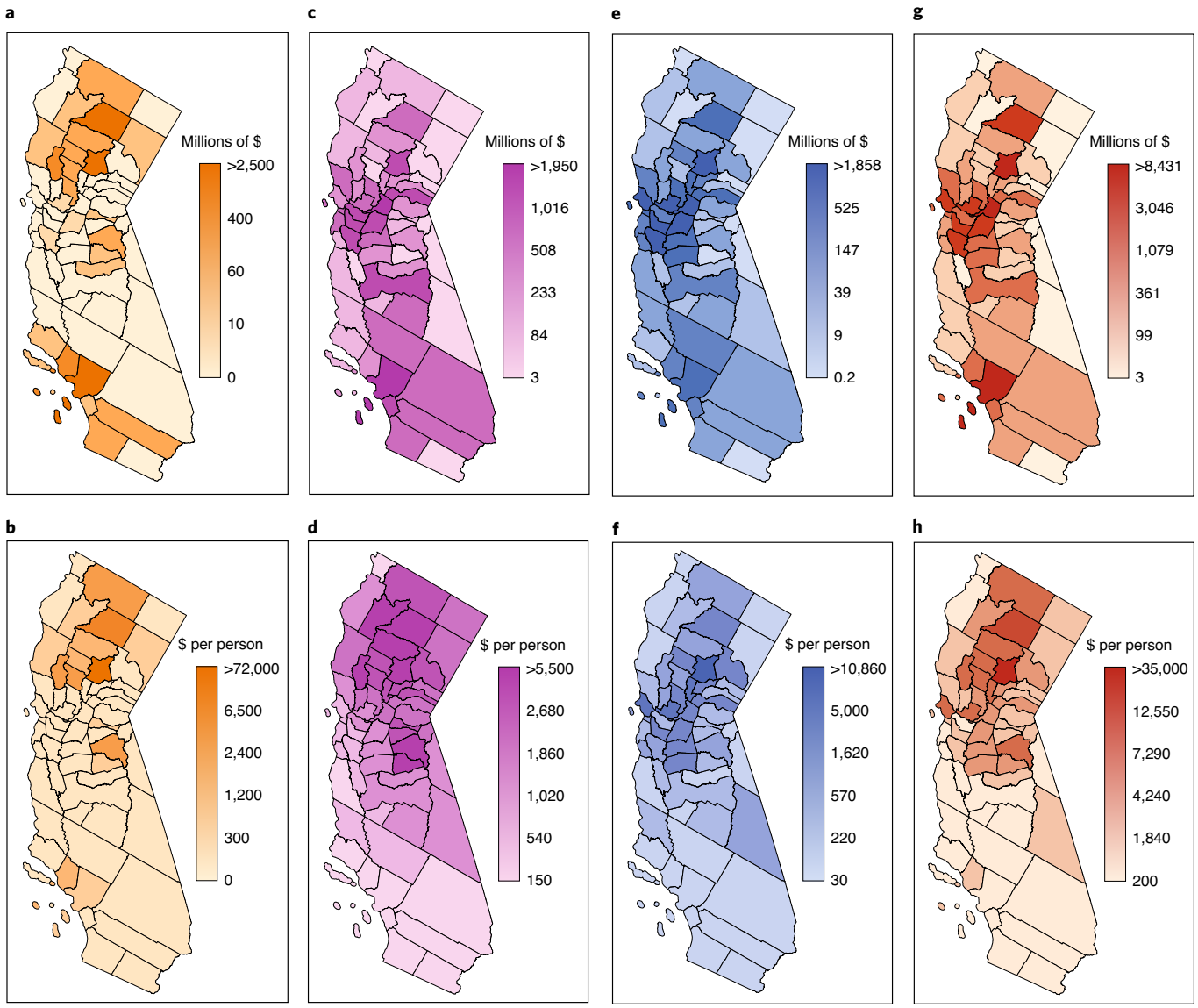

Fig. 2 | Fire-related damages from the 2018 wildfires in California. a, County-level capital loss. **b**, Capital loss per capita. **c**, County-level health cost. **d**, Health cost per capita. **e**, County-level indirect loss. **f**, Indirect loss per capita. **g**, County-level total damages. **h**, Total damages per capita. Data for county boundary lines from the Geography Program of the United States Census Bureau (www.census.gov/programs-surveys/geography.html).

categories, the geographical distribution of total losses is substantial in many California counties, although often for different reasons (Fig. 2g and Supplementary Fig. 2). Total losses were again largest in Butte County ($23.2 billion), followed by Sacramento and Los Angeles counties ($10.1 and $9.1 billion, respectively; Supplementary Table 1). Per capita losses highlight areas with relatively low populations but large losses; in Butte, Shasta and Lake counties, damages were $101,000, $35,000 and $13,000 per capita, respectively (Fig. 2h and Supplementary Table 1).

The ternary plots in Fig. 3 show the magnitude of 2018 fire impacts on specific industry sectors in California (size of circles) as well as the relative shares of capital losses, health costs and indirect losses (position of circles; see also Supplementary Table 2). The service industry suffered the greatest total losses ($44.4 billion, or 45.1% of the statewide total), with 44.7% of this total related to health costs, 33.8% related to capital losses and 21.5% associated with indirect losses (red circle in Fig. 3a). By contrast, 78.1% of damages to the manufacturing sector (second largest at $22.3 billion, 22.6% of total losses) were indirect losses, with just 15.7% in health costs and 6.2% in capital losses (turquoise circle in Fig. 3a). Combined losses in all of the other five major sectors were $31.7 billion (Fig. 3a). Yet, breaking damages into subsectors, we see the composition of damages varies widely. For example, in the service sector, damages to the real estate industry were heavily concentrated in capital losses (77.2% of the subsector's $9.3 billion in damages) as opposed to mostly health costs in labour-intensive subsectors such as education, software and restaurants (Fig. 3b) and trade (retail) subsectors (Fig. 3d). Damages to some manufacturing subsectors were also mostly health costs (for example, the aircraft, medical and electrical industries), but overall damages are dominated by indirect losses related to the chemical industry (Fig. 3c). The chemical industry is the largest manufacturing sector in California and contributes about 3.7% of overall statewide GDP. The figure in some counties, such as Solano and Contra Costa, accounts for 25–29% of county-level industrial outputs. During the fire events, the chemical industry suffered direct capital loss of $284.5 million and health costs of $375.1 million, but the changes of demand and supply patterns in chemical production chains caused indirect loss within

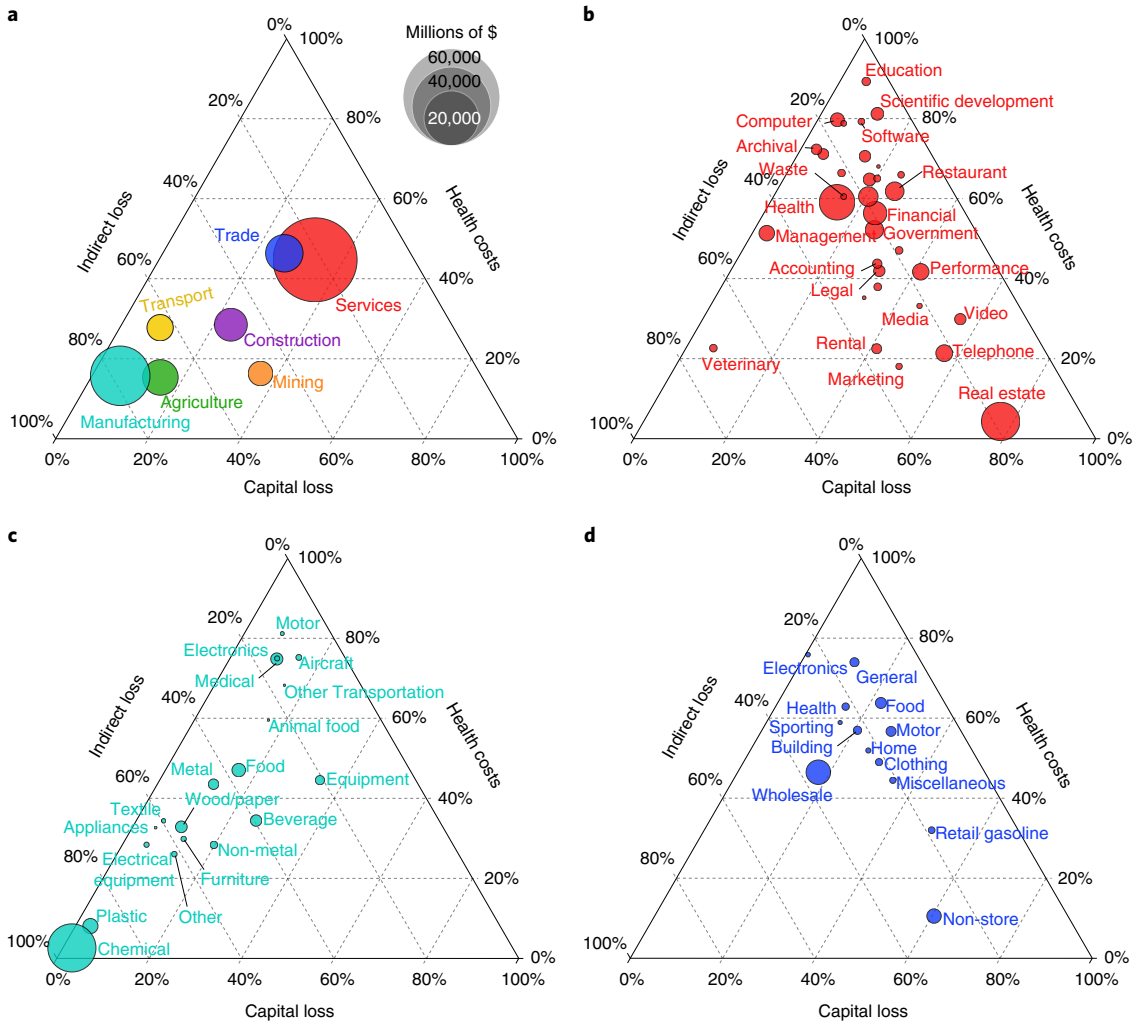

Fig. 3 | Impacts of wildfires on specific industry sectors in California. a, Ternary plot shows the magnitude of 2018 fire impacts on specific industry sectors in California (size of circles) as well as the relative shares of capital losses, health costs and indirect losses (position of circles). **b**–**d**, Ternary plots show the losses in each subsector in services (**b**), manufacturing (**c**) and trade (**d**). See Supplementary Figs. 5–8 and Supplementary Table 2 for damages in other subsectors.

the state of $13,639.3 million and out of state of $2,513.1 million. Supplementary Figs. 4–7 and Supplementary Table 2 show and further explore subsector results for each of the other major sectors.

Uncertainties. *Sensitivity analysis of parameters in epidemiological model.* We perform a Monte Carlo analysis with BenMAP Community Edition (BenMAP-CE) to quantify the 95% confidence interval (CI) around the mean incidence and valuation estimates. Although long-term changes in $PM_{2.5}$ exposure dominate the valuation impacts, we report results for both short-term and long-term exposure related to the 2018 wildfire episodes. Consistent with the current modelling methods practiced by regulatory agencies, including the US Environmental Protection Agency and South Coast Air Quality Management District, no concentration threshold is assumed for the health impact assessment modelling[21]. Statewide, mean health costs of the fires are $32.15 billion, and 95% CIs range from $13.33 billion to $75.92 billion. The range of uncertainty in our valuation is generally consistent with other BenMAP estimates reported in the literature and relates to statistical error and cross-study variability[21–23].

Uncertainties in capital damage statistics. The uncertainty in capital damage statistics is related mostly to the degree of building losses and their reconstruction costs. Since the degree of damage to affected buildings is not given by official reports, we assume the average damage proportion is 50%, but with a range uniformly distributed from 1% to 99%. For the reconstruction cost of buildings in different regions in California, we refer to values reported by Allstate, CoreLogic and reinsurance companies (that is, Munich RE[15]). These companies' *Insurance Journal* reports provide the number and total reconstruction cost value of buildings within the perimeters of the major fires. We then calculate the average reconstruction cost of the buildings in different regions using these valuations. We find an average reconstruction cost for residential buildings of $238,600 in the Camp fire area and $695,500 in the Woolsey fire area. For commercial buildings, the average is $2.69 million in the Camp fire area and $1.04 million in the Woolsey fire area. We use these two fires to bound building reconstruction costs in other regions, randomly selecting from the full range for Monte Carlo simulations to create a distribution of capital losses. In this way, we find the average total damage to residential buildings is $4.52 billion, with a 95% CI from $3.13 billion to $7.49 billion, and the average total damage to commercial buildings is $23.2 billion, with a 95% CI from $15.78 billion to $29.62 billion.

Sensitivity analysis of parameters in the economic model. There are two main parameters in the economic model that will bring

uncertainty to the results. One is the reconstruction time of the building, and the other is the time of traffic recovery in the fire area. We assume the average recovery time of a building is 90 days; that is, it takes 90 days from the acquisition of recovery resources to complete rebuilding. This rebuilding time parameter is then varied from 60 days to 120 days in our sensitivity analysis. Similarly, we assume that the average recovery time of transportation in a fire area was 14 days after the fire was contained and vary this parameter from 7 days and 21 days in the sensitivity analysis. In this way, we find that the average production loss is $88.61 billion, ranging from $79.40 billion to $96.05 billion.

Sensitivity analysis of total economic footprint. Using the distribution of losses obtained by our three types of losses uncertainty analysis, we perform 2,000 simulations in our Monte Carlo analysis to generate a distribution of the total economic footprint of California wildfires in 2018. Supplementary Fig. 8 shows the resulting distribution of total fire losses along with 95% CIs: $148.5 billion, ranging from $126.07 billion to $192.93 billion.

Discussion

Although substantial, the direct capital losses related to the 2018 California wildfires represent only 27.0% of the statewide total damages we estimate in this study, and an even smaller share of the impacts in some counties and to specific industry sectors. Health costs and indirect economic losses, rarely if ever quantified before, represent an enormous 31.5% and 41.5% of the statewide total damages, respectively. Moreover, these indirect impacts in some case fell heavily on locations (for example, Sacramento County) and industries (for example, chemical manufacturing) away from major fires. In the same way, our results reveal that the United States beyond California also suffered considerable economic damages ($45.9 billion) related to California's wildfires. Quantifying and mapping these less obvious but large damages in 2018 leads to the conclusion that large wildfires occurring in California or other western states are not isolated problems. Although the horrific scenes of death and destruction may seem confined to specific communities, the related economic and health impacts affect a much broader area, which in 2018 included substantial losses to the national economy. Recognizing the full magnitude and scope of wildfires' economic footprint may in turn influence decision making about land and forest management, fire suppression efforts and development patterns. For example, health costs and indirect losses of future fires might be reduced by focusing fire prevention efforts on areas typically upwind of major population centres or near important industrial or transportation infrastructure. Similarly, our results suggest that the indirect economic losses related to the recent forced electricity outages[24,25] might be much larger than the capital losses that may have been avoided (although lives may have been saved).

The magnitude and spatial distribution of wildfire impacts support greater investments in fire prevention and suppression, including investments by jurisdictions indirectly affected by the related pollution and economic disruption. Our work forcefully demonstrates that the impacts of wildfires are much more broadly distributed in space than conventional wisdom might suggest. Now and as the climate changes, wildfire risks transcend far beyond the wildland–urban interface; they are a statewide and regional challenge. In turn, recognizing the greater magnitude and far-reaching indirect impacts of the recent fires may justify dedicating substantially greater resources to mitigating fire risks and coordinating planning and responses across the state and region.

However, our estimates of wildfire-related damages in 2018 are subject to some important uncertainties, and our methods may not capture all types of economic damages. For example, the reconstruction cost value of buildings damaged in fire events and to be restored after the disaster are based on average estimates of each fire region rather than on specific marketing information. Similarly, estimates of health costs assume methods that reasonably account for statistical uncertainties but may understate the impact of epistemic uncertainties, including those associated with air quality modelling, epidemiological science and health economic valuation[26]. Furthermore, only impacts to California populations are quantified although intrastate transport of pollutants may accrue health costs elsewhere. Time lags between the fires and the restoration of transportation lines, as well as the time required to rebuild are the key uncertain parameters in estimating indirect losses. Our analysis also neglects international trade and difficult-to-quantify impacts such as effects on mental health and the prospect of cascading events such as subsequent landslides. Unfortunately, indirect economic costs are extraordinarily difficult to validate[11,18] because models such as ours focus on estimating fire-related supply-chain losses assuming that the myriad other factors that affect economic growth do not change, but the reality is that many such other factors will have changed, and the growth of the state's GDP will be the net of all these changes. In an effort to quantify some of the uncertainties, we conducted a sensitivity analysis for each of three models used in the study and integrated the results into a single uncertainty analysis of the overall economic footprints. Details are available in the Methods and Supplementary Information. Despite the uncertainties, projected climate change, population growth and economic development will continue to increase wildfire risks in California and the rest of the western United States in the years and decades to come. Understanding the economic footprint of past fires can only help in strategically confronting these risks so as to cost-effectively minimize the impacts of future fires.

Methods

Definition of the economic footprint of wildfires. The economic footprint of a wildfire provides a comprehensive accounting of the wildfire-induced direct and indirect economic losses in our socioeconomic system. The economic footprint of a wildfire consists of (1) the direct capital cost (the cost to repair or reconstruct the assets that have been damaged or destroyed in the wildfires); (2) the health cost (medical costs, working time loss and rising mortality due to air pollution induced by wildfires); (3) the indirect cost (the potential value-added losses of the economy due to the supply-chain disruptions triggered by wildfires). Note that the indirect part of the economic footprint of wildfires was designed to estimate the potential supply-chain losses related to the wildfires assuming that other factors do not change. As such, the analytical framework is fundamentally different from those used in other macroeconomic analyses that aim to simulate and project real changes in an economy.

Supplementary Fig. 9 shows the overall analytical framework for economic footprint accounting. A random forest model was used to estimate the daily mean $PM_{2.5}$ concentration at 4 km spatial resolution over California (Supplementary Fig. 9a). Then, we used two GEOS-Chem simulations (without and with fire emissions) to calculate the fraction of wildfire-induced $PM_{2.5}$ emission (Supplementary Fig. 9b). With the estimated gridded pollutant concentration data and population density data as inputs, we used the environmental BenMAP-CE version 1.5 to assess the health-related socioeconomic costs attributable to the degradation of air quality from wildfire emissions (Supplementary Fig. 9c). We estimated the losses of capital stock, both productive capital and residential building losses, according to reports on fires by CAL Fire and reports on reconstruction cost by insurance companies (Supplementary Fig. 9d). Finally, we used an MRDF model to simulate the ripple effect of fire-induced production time loss, capital loss and traffic disruption on supply-chain networks and assess indirect economic losses (Supplementary Fig. 9e).

Wildfire-induced air pollution estimation. Daily mean $PM_{2.5}$ concentrations at 4 km spatial resolution over California used in this study were estimated using random forest models that incorporated information from multiple sources, including ground measurements, satellite remote sensing, chemical transport model simulations, meteorological fields and land use variables. This method was widely used in previous studies on estimating high-resolution full-coverage $PM_{2.5}$ concentrations (for example, Xiao et al.[27]) and was able to capture large fire events[28].

Ground-level $PM_{2.5}$ measurements for 2018 were obtained from the US Environmental Protection Agency's Air Quality System (see Data availability). Satellite-based aerosol optical depth (AOD) data retrieved by the multi-angle implementation of atmospheric correction (MAIAC) algorithm at 1 km spatial resolution[29,30] on the basis of the Moderate Resolution Imaging Spectroradiometer

(MODIS) were downloaded from NASA Earthdata portal. $PM_{2.5}$ simulations from the Modern-Era Retrospective analysis for Research and Applications, version 2 (MERRA-2) at 0.5°×0.625° resolution were also used in this study as additional information on $PM_{2.5}$ distribution. Other variables compiled in this study included pressure, temperature, wind speed, specific humidity, precipitation, shortwave and longwave fluxes, and evaporation at ~13 km spatial resolution from the North American Land Data Assimilation Systems; elevation at 30 m spatial resolution from the National Elevation Dataset; forest cover, shrub cover and cultivated land cover at 30 m spatial resolution from the 2011 National Land Cover Database; road lengths of major roads, highways and interstate highways extracted from ESRI StreetMap USA (Environmental Systems Research Institute); and population data from 2017 LandScan data. All data were integrated into the 1 km MAIAC grid, and the $PM_{2.5}$ concentrations were first estimated at 1 km and then aggregated into a 4 km grid.

In general, the random forest algorithm is an ensemble learning method based on decision trees, which has the advantage of allowing both continuous and categorical input variables and is quite robust to outliers. It also provides variable importance rankings as well as out-of-bag errors for variable selection and model evaluation. We built two random forest models in this study (with and without satellite inputs) and then merged their predictions to obtain full spatial and temporal coverage of $PM_{2.5}$ data, since AOD has missingness in certain times and places. Our models produced good results, with out-of-bag R^2 of 0.83 and 0.80 for the two models, respectively.

When using AOD to estimate $PM_{2.5}$ concentrations, statistical models (for example, multilinear regression, geographically weighted regression, generalized additive model) or machine-learning models were built to explain the spatial–temporal varied relationship between AOD and $PM_{2.5}$ at locations where $PM_{2.5}$ monitors are available, as follows:

$$PM_{2.5,obs} = f(AOD, \text{ancillary data})$$

where the independent variable $PM_{2.5,obs}$ is $PM_{2.5}$ observations; AOD is the satellite AOD at corresponding locations; and ancillary data includes meteorological conditions, land use variable and other parameters that could influence the relationship between AOD and $PM_{2.5}$. Then $PM_{2.5}$ concentrations outside monitoring locations could be predicted by AOD and the ancillary data. Since AOD is randomly missing due to cloud cover and snow cover, we also built a model using MERRA-2 data at locations where AOD is unavailable:

$$PM_{2.5,obs} = f(PM_{2.5,MERRA\text{-}2}, \text{ancillary data})$$

Results from the two models are merged to get the final results without double counting.

Note that this method provides total surface $PM_{2.5}$ from all emission sources but cannot identify the part specifically contributed by wildfire emissions. We therefore use a second model (GEOS-Chem) to simulate the fraction of $PM_{2.5}$ induced by wildfires in total $PM_{2.5}$. To calculate the wildfire-induced $PM_{2.5}$ fractions, we used two GEOS-Chem model scenarios—with and without fire emissions. The differences between these two scenarios divided by the total $PM_{2.5}$ were calculated as the wildfire $PM_{2.5}$ fractions. The fire emissions used in this study were GFED4s emissions[16]. The GFED4 emissions used in this study are at spatial resolution of 0.25°×0.25° and temporal resolution of 3-hourly. Our global GEOS-Chem model has a spatial resolution of 2°×2.5°. The transport/convection time step in the model is 600 seconds and the chemistry/emission time step is 1,200 seconds. Secondary organic aerosols are included in our model with the simple secondary-organic-aerosol scheme that provides the correct amount of global secondary organic aerosol without detailed chemistry.

Health impact assessment. A deep breadth of scientific literature demonstrates a positive association between exposure to ambient outdoor air pollution and increases in the incidence of morbidity and mortality within exposed populations[31–33]. Health-related socioeconomic costs attributable to the degradation of air quality from wildfire emissions was assessed using the environmental BenMAP-CE version 1.5[17]. BenMAP-CE is an open-source software developed by the US Environmental Protection Agency and is widely used in emission regulation assessment[34,35] and wildfire health impact evaluation[36,37]. BenMAP applies the relationship between the pollution and certain health effects, which is often referred to as the health impact function or the concentration–response (C–R) function (derived from epidemiology studies; Supplementary Fig. 10). The variables that appear in health impact functions are the following: air quality change (Delta), the difference between the starting air pollution level (baseline) and the air pollution level after some change (control); health effect estimate (β), an estimate (obtained from epidemiology studies) of the percentage change in the risk of an adverse health effect due to changes in ambient air pollution; exposed population, the number of people that are in the region where we are assessing the air pollution reduction; health baseline incidence, an estimate of the average number of people who die (or suffer from some adverse health effect) in a given population over a given period.

BenMAP also calculates the economic value of avoided health effects. After calculating the health changes, one can estimate the economic value by multiplying the reduction of the health effect by an estimate of the economic value per case, which is obtained from health economic studies. In Supplementary Fig. 11 is a flow diagram with all the data needed to obtain final monetary benefit results.

BenMAP-CE utilizes as an input the concentration differences resolved at the 24-hour time step for $PM_{2.5}$ between the baseline (without wildfire) and the control case (with wildfire) determined in Methods subsection 'Wildfire-induced air pollution estimation' (with daily based concentration). Population projections are based on suggested BenMAP practices using Landscan data at 1 km spatial resolution[38] for the year 2018 and downscaled to the 4 km study domain using geospatial modelling. Baseline incidence rates at the county level by five-year age groups are obtained as appropriate for the current California population and include estimates from public administrative records when possible[39]. C–R functions are used to quantify the increased incidence of mortality and morbidity endpoints resulting from increases in $PM_{2.5}$ and are selected from a systematic review of the epidemiological literature accounting for applicability criteria, including (among others) study date and design and geography and population characteristics[40,41]. For example, all-cause mortality effects associated with increases in annual $PM_{2.5}$ exposure were quantified by pooling C–R functions from Jerrett et al.[42] and Krewski et al.[43]. We use baseline incidence rates for mortality provided by the South Coast Air Quality Management District taken from local health data based on public administrative data wherever possible[39], and then calculate the additional incidence occurring from increased pollutant exposure. Socioeconomic costs are then estimated using willingness-to-pay and cost-of-illness valuation functions from a survey of health economic literature for mortality and morbidity[44,45]. The value of statistical life selected for application with avoided incidents of mortality was $9 million as a midpoint of a range of $4.2 million to $13.7 million from Robinson and Hammitt[46], all expressed in US$$_{2013}$ and based on 2013 income levels, as recommended by Industrial Economics and Lisa Robinson[45].

Capital damages estimation. The estimation of capital damages requires mainly two types of basic data: the number of each type of building damaged or destroyed by wildfires and the repair or reconstruction cost of these structures. The former is derived mainly from the National Large Incident Year-to-Date Report[14] issued by the National Interagency Fire Center of the United States. The California Fire official website provides more detailed statistics or maps for some major wildfires. For the reconstruction cost of buildings in different parts of California, we refer to Allstate[47], Corelogic[48] and Munich RE[15]. Their reports in *Insurance Journal* provide the number and total reconstruction cost value of buildings within the perimeter of the major fires. We used this information to calculate the average reconstruction cost of the buildings in different regions. For the damaged structures, we assume that the repair cost of partially damaged structures is 50% of their reconstruction cost, and this ratio ranges from 1% to 99% in the uncertainty analysis.

Indirect economic impact assessment. The direct losses are used as negative shocks of our MRDF model to assess the indirect economic impact of wildfires on the economic system. The MRDF model is an extension of the adaptive regional input–output model proposed by Hallegate[18], which has been widely used in disaster impact assessment[11,19,20] due to its ability to consider both changes in production capacity due to productive capital losses and adaptive behaviour in disaster aftermaths simultaneously in the IO framework. We extend the adaptive regional input–output model to a multiregional case on the basis of the multiregional input–output (MRIO) analysis and the linear programming (LP) technique. Linking the improved model with the latest MRIO table for California, we assessed the output losses of industrial sectors in different regions caused by the supply-chain disruption triggered by the initial wildfire shocks.

To estimate the indirect costs of wildfires under the input–output framework, we first compiled an MRIO table for the study subjects. There are 59 regions in the MRIO table, including 58 counties in California and an aggregation region (the rest of United States). Production activities in each region are divided into 80 industrial sectors (Supplementary Table 3), and each sector produces one unique commodity. The basic data required to create the raw MRIO table came from IMPLAN, including the regional input–output table, the import matrix for each county and the rest of the United States, and the trade-flow data for each commodity between the regions. We use the 'Chenery–Moses' approach[49] for consistent estimation of the intra- and interregional transections and the RAS method for balancing the raw MRIO table.

We assume that the economy before the wildfires is in a stable state and can be expressed by equation (1), the standard open input–output model developed by Leontief:

$$\mathbf{x} = A\mathbf{x} + \mathbf{f} \quad (1)$$

where $\mathbf{x}$ is a column vector of dimension $N \times M$ (where M is the number of industrial sectors and N is the number of regions) representing the total production of each industrial sector in each region, $A\mathbf{x}$ represents the intermediate demand vector, where each element of the matrix A, $[a_{rsij}]$, refers to the technical relation showing product i in region r needed to produce one unit of product j in region s and $\mathbf{f}$ indicates the final demand vector of products. This standard model exactly replicates the equilibrium without disruptions.

When an economy is hit by a disaster, some part of its productive capacity is lost due to productive constraints, including productive capital loss, productive time loss and transportation constraints. These constraints will first lead to production declines of industrial sectors directly affected by the disaster, and then this initial production decline can trigger both forward and backward effects[19,20] through the intra- and interregional industrial linkages.

Another important aspect to model the disaster aftermath is the reconstruction demand from the affected economy. Producers affected by the disaster directly want to restore their production capacity by reconstructing their destroyed buildings or repairing their damaged buildings. To do that, industrial sectors need reconstruction resources from the construction sector and the manufacturing sector. Following Hallegate[18,19], we assume that damages in each sector create an additional demand of 75% of the damage value to the construction sector and of 25% of the damage value to the manufacturing sector. The reconstruction demand (RD) of industry i in region r to industry j in region s, $f^{RD}_{r,s,i,j,t}$, can be calculated as follows:

$$f^{RD}_{r,s,i,j,t} = \begin{cases} 0, & k^{\Delta}_{r,i,t} \geq k_{r,i,0} \\ d_j \times \left(k_{r,i,0} - k^{\Delta}_{r,i,t}\right) \times \frac{x_{s,j,t}}{\sum_{ss,jj} x_{ss,jj,t}}, & k^{\Delta}_{r,i,t} < k_{r,i,0} \end{cases}$$

where t denotes time, $i,j = 1,\ldots M$ (M denotes the number of sectors) and $r,s = 1,\ldots,N$ (N denotes the number of regions), $k^{\Delta}_{r,i,t}$ denotes capital stock of industrial sector i in region r in time step t, d_j denotes the distribution coefficients and $x_{s,j,t}$ denotes the output of industrial sector j in region s in time step t.

We assume that each industry sector will try its best to meet the demands from its clients under the current constraints. An LP technique is used to represent the production behaviour of industrial sectors with productive capacity constraints in each period[50]. The LP problem can be described by the following set of equations. A full list of all variables and their descriptions can be found in Supplementary Table 4.

$$\max i' x_t = \sum_{s,j} x_{s,j,t} \tag{2}$$

subject to the following production-side constraints (1–4):

(1) the production technology constraints (the production functions):

$$x_{s,j,t} = \min\left\{\forall i, \frac{z_{r,s,i,j,t}}{a_{r,s,i,j}}; \forall u, \frac{v_{u,s,j,t}}{b_{u,s,j}}\right\} \tag{3}$$

(2) the productive capital constraints:

$$v_{k,s,j,t} \leq \left(\frac{k_{s,j,t}}{k_{s,j,0}}\right) \times v_{k,s,j,0} \tag{4}$$

(3) the working time constraints:

$$v_{l,s,j,t} \leq \left(\frac{l_{s,j,t}}{l_{s,j,0}}\right) \times v_{l,s,j,0} \tag{5}$$

(4) the transportation constraints:

$$z_{r,s,i,j,t} \leq \left(\frac{p_{r,t}}{p_{r,0}}\right) \times z_{r,s,i,j,0} \tag{6}$$

and the following demand-side constraints:

(5) the intermediate demand constraints:

$$\sum_{r,i} z_{r,s,i,j,t} \leq x_{s,j,t} \tag{7}$$

(6) the total demand constraints:

$$x_{s,j,t} \leq \sum_{r,i} z_{r,s,i,j,t} + \sum_{r} f^{D}_{r,s,j,t} + \sum_{r,i} f^{RD}_{r,s,i,j,t} \tag{8}$$

where $z_{r,s,i,j,t}$ denotes the intermediate demand of industry i in region r to industry j in region s and $f^{D}_{r,s,j,t}$ denotes the final demand of households in region r to industry j in region s. The solution of the LP problem determined the output of each sector in each region, that is, $x_{s,j,t}$, which will be distributed into first the intermediate consumption demand, which is determined in the LP solution, and then other demand, that is, final demand and reconstruction demand. If the output of an industrial sector cannot meet the demands from its clients, a proportional rationing scheme will be applied[18,19]. The products will be allocated to the clients according to their proportion of demand.

In our improved model, production capacity will not be restored immediately as the reconstruction resources are filled, but with some delay. Reconstruction of the production plant takes time. We record the recovered resources as construction in progress, which did not play any role in the production process. The average time to build a building in California is about 4–8 months. Considering that the speed of post-disaster reconstruction may be faster than usual, in this study, we made a less severe assumption that the construction of the buildings will take 90 days. In other words, the corresponding production capacity will be restored after the reconstruction resources are received.

The dynamic of another two supply-side constraints is modelled as follows: for transportation, we assume that transportation in the area directly affected by fires will be disrupted immediately, and the lockdown will gradually be released within the next few days. For labour, the availability of labour is constrained by transportation disruption and fire-pollution-induced disease admission. The former is parallel with the transportation disruption, and the latter is derived from the simulation results of BenMAP.

The economy will recover to the pre-disaster equilibrium after all constraints are lifted. We define the value-added decrease of each industrial sector in a network caused by an exogenous negative shock as the disaster impacts of the shock. Note that we aim to assess the potential losses due to only the wildfires. Therefore, other factors (for example, technology) remain unchanged. In this way, we separately extract the effects of disaster shocks. The indirect economic cost, EC, is calculated as follows:

$$EC_{s,j} = \sum_{u} v_{u,s,j,0} \times T - \sum_{u,t} v_{u,s,j,t}$$

where T represents the total time step used to recover to the pre-crisis equilibrium, and u presents the type of primary inputs, l or k.

Data availability

Ground-level $PM_{2.5}$ measurements for 2018 were obtained from US Environmental Protection Agency's Air Quality System (https://www.epa.gov/outdoor-air-quality-data/); MAIAC AOD was downloaded from NASA Earthdata portal (https://search.earthdata.nasa.gov/); North American Land Data Assimilation Systems, elevation at 30 m spatial resolution is from the National Elevation Dataset (NED, http://ned.usgs.gov); forest cover, shrub cover and cultivated land cover at 30 m spatial resolution is from the 2011 National Land Cover Database (NLCD, http://www.mrlc.gov); road lengths of major roads, highways and interstate highways was extracted from ESRI StreetMap USA (Environmental Systems Research Institute); the population data are from 2017 LandScan data (https://landscan.ornl.gov/downloads/2017); wildland fire information is from the National Interagency Fire Center (National Large Incident Year-to-Date Report 2018), CAL FIRE (https://www.fire.ca.gov/); the county-level input–output table and trade-flow data between counties are from IMPLAN (https://implan.com/data/).

Code availability

The simulation code for the indirect economic costs can be accessed at https://github.com/DaopingW/Disaster-Footprint-Model. The minimal input for the code is the multiregional input–output table. The sample code and test data for the minimal inputs are also provided.

Received: 9 March 2020; Accepted: 27 October 2020;
Published online: 7 December 2020

References

1. Abatzoglou, J. T. & Williams, A. P. Impact of anthropogenic climate change on wildfire across western US forests. *Proc. Natl Acad. Sci. USA* **113**, 11770–11775 (2016).
2. Dennison, P. E., Brewer, S. C., Arnold, J. D. & Moritz, M. A. Large wildfire trends in the western United States, 1984–2011. *Geophys. Res. Lett.* **41**, 2928–2933 (2014).
3. Holden, Z. A. et al. Decreasing fire season precipitation increased recent western US forest wildfire activity. *Proc. Natl Acad. Sci. USA* **115**, E8349 (2018).
4. Kitzberger, T., Falk, D. A., Westerling, A. L. & Swetnam, T. W. Direct and indirect climate controls predict heterogeneous early-mid 21st century wildfire burned area across western and boreal North America. *PLoS ONE* **12**, e0188486 (2017).
5. Latif, M. T. et al. Southeast Asian forest fires (1997/1998): El Niño as a driver of regional impacts. *Air Pollut. Epis.* **6**, 191–225 (2017).
6. Balch, J. K. et al. Human-started wildfires expand the fire niche across the United States. *Proc. Natl Acad. Sci. USA* **114**, 2946–2951 (2017).
7. Radeloff, V. C. et al. Rapid growth of the US wildland–urban interface raises wildfire risk. *Proc. Natl Acad. Sci. USA* **115**, 3314–3319 (2018).
8. Zhuang, J., Payyappalli, V. M., Behrendt, A. & Lukasiewicz, K. *Total Cost of Fire in the United States* (Fire Protection Research Foundation, 2017).
9. Shi, H. et al. Modeling study of the air quality impact of record-breaking Southern California wildfires in December 2017. *J. Geophys. Res. Atmos.* **124**, 6554–6570 (2019).
10. Reid Colleen, E. et al. Critical review of health impacts of wildfire smoke exposure. *Environ. Health Perspect.* **124**, 1334–1343 (2016).
11. Inoue, H. & Todo, Y. Firm-level propagation of shocks through supply-chain networks. *Nat. Sustain.* **2**, 841–847 (2019).
12. Rose, A., Benavides, J., Chang, S. E., Szczesniak, P. & Lim, D. The regional economic impact of an earthquake: direct and indirect effects of electricity lifeline disruptions. *J. Reg. Sci.* **37**, 437–458 (1997).

13. Johnston Fay, H. et al. Estimated global mortality attributable to smoke from landscape fires. *Environ. Health Perspect.* **120**, 695–701 (2012).
14. *2018 National Year-to-Date Report on Fires and Acres Burned* (National Interagency Fire Center, 2018).
15. Faust, E. & Steuer, M. Climate change increases wildfire risk in California. *Munich RE* (26 March 2019); https://go.nature.com/35nKs2b
16. Randerson, J. T., Van Der Werf, G. R., Giglio, L., Collatz, G. J. & Kasibhatla, P. S. *Global Fire Emissions Database* Version 4.1 (GFEDv4) (ORNL Distributed Active Archive Center, 2017); https://doi.org/10.3334/ORNLDAAC/1293
17. Sacks, J. D. et al. The environmental benefits mapping and analysis program—community edition (BenMAP–CE): a tool to estimate the health and economic benefits of reducing air pollution. *Environ. Model. Softw.* **104**, 118–129 (2018).
18. Hallegatte, S. An adaptive regional input–output model and its application to the assessment of the economic cost of Katrina. *Risk Anal.* **28**, 779–799 (2008).
19. Hallegatte, S. Modeling the role of inventories and heterogeneity in the assessment of the economic costs of natural disasters. *Risk Anal.* **34**, 152–167 (2014).
20. Guan, D. et al. Global supply-chain effects of COVID-19 control measures. *Nat. Hum. Behav.* **4**, 577–587 (2020).
21. Shen, E., Oliver, A. & Dabirian, S. *Final Socioeconomic Report Appendices to the 2016 Air Quality Management Plan* (South Coast Air Quality Management District, 2017); https://go.nature.com/3ePpwEj
22. Davidson, K., Hallberg, A., McCubbin, D. & Hubbell, B. Analysis of $PM_{2.5}$ using the environmental benefits mapping and analysis program (BenMAP). *J. Toxicol. Environ. Health A* **70**, 332–346 (2007).
23. *Benefits and Costs of the Clean Air Act 1990–2020, the Second Prospective Study* (US Environmental Protection Agency, 2011); https://go.nature.com/3f3muwp
24. Jazebi, S., León, F. D. & Nelson, A. Review of wildfire management techniques—part I: causes, prevention, detection, suppression, and data analytics. *IEEE Trans. Power Deliv.* **35**, 430–439 (2020).
25. Roberts, D. California's deliberate blackouts were outrageous and harmful. They're going to happen again. *Vox* (24 October 2019); https://go.nature.com/3lpnL34
26. Smith, A. E. & Gans, W. Enhancing the characterization of epistemic uncertainties in $PM_{2.5}$ risk analyses. *Risk Anal.* **35**, 361–378 (2015).
27. Xiao, Q., Chang, H. H., Geng, G. & Liu, Y. An ensemble machine-learning model to predict historical $PM_{2.5}$ concentrations in China from satellite data. *Environ. Sci. Technol.* **52**, 13260–13269 (2018).
28. Stowell, J. D. et al. Associations of wildfire smoke $PM_{2.5}$ exposure with cardiorespiratory events in Colorado 2011–2014. *Environ. Int.* **133**, 105151 (2019).
29. Lyapustin, A., Martonchik, J., Wang, Y., Laszlo, I. & Korkin, S. Multiangle implementation of atmospheric correction (MAIAC): 1. radiative transfer basis and look-up tables. *J. Geophys. Res. Atmos.* https://doi.org/10.1029/2010JD014985 (2011).
30. Lyapustin, A. et al. Multiangle implementation of atmospheric correction (MAIAC): 2. aerosol algorithm. *J. Geophys. Res. Atmos.* https://doi.org/10.1029/2010JD014986 (2011).
31. Chen, H., Goldberg, M. S. & Villeneuve, P. J. A systematic review of the relation between long-term exposure to ambient air pollution and chronic diseases. *Rev. Environ. Health* **23**, 243–297 (2008).
32. Kampa, M. & Castanas, E. Human health effects of air pollution. *Environ. Pollut.* **151**, 362–367 (2008).
33. Pascal, M. et al. Assessing the public health impacts of urban air pollution in 25 European cities: results of the Aphekom project. *Sci. Total Environ.* **449**, 390–400 (2013).
34. Driscoll, C. T. et al. US power plant carbon standards and clean air and health co-benefits. *Nat. Clim. Change* **5**, 535–540 (2015).
35. Zhu, S., Horne, J. R., Mac Kinnon, M., Samuelsen, G. S. & Dabdub, D. Comprehensively assessing the drivers of future air quality in California. *Environ. Int.* **125**, 386–398 (2019).
36. Jones, B. A., Thacher, J. A., Chermak, J. M. & Berrens, R. P. Wildfire smoke health costs: a methods case study for a Southwestern US 'mega-fire'. *J. Environ. Econ. Policy* **5**, 181–199 (2016).
37. Jones, B. A. & Berrens, R. P. Application of an original wildfire smoke health cost benefits transfer protocol to the western US, 2005–2015. *Environ. Manage.* **60**, 809–822 (2017).
38. Rose, A. N., McKee, J. J., Urban, M. L. & Bright, E. A. *LandScan* (Oak Ridge National Laboratory, 2018).
39. Marrison, H., Penn, S. & Roman, H. *Review of Baseline Incidence Rate Estimates for Use in 2016 Socioeconomic Assessment* (Industrial Economics, 2016); https://go.nature.com/36tSOEt
40. *Literature Review of Air Pollution-Related Health Endpoints and Concentration–Response Functions for Particulate Matter: Results and Recommendations* (Industrial Economics, 2016); https://go.nature.com/35n6cLg
41. *Literature Review of Air Pollution-Related Health Endpoints and Concentration–Response Functions for Ozone, Nitrogen Dioxide, and Sulfur Dioxide: Results and Recommendations* (Industrial Economics, 2016); https://go.nature.com/38xDWaY
42. Jerrett, M. et al. Spatial analysis of air pollution and mortality in California. *Am. J. Respir. Crit. Care Med.* **188**, 593–599 (2013).
43. Krewski, D. et al. Extended follow-up and spatial analysis of the American Cancer Society study linking particulate air pollution and mortality. *Res. Rep. Health Eff. Inst.* **140**, 5–136 (2009).
44. Roman, H., Marrison, H. & Robinson, L. *Review of Morbidity Valuation Estimates for Use in 2016 Socioeconomic Assessment* (Industrial Economics, 2016); https://go.nature.com/2UmrmmF
45. Roman, H. & Robinson, L. *Review of Mortality Risk Reduction Valuation Estimates for 2016 Socioeconomic Assessment* (Industrial Economics, 2016); https://go.nature.com/32xA8mj
46. Robinson, L. A. & Hammitt, J. K. Valuing reductions in fatal illness risks: implications of recent research. *Health Econ.* **25**, 1039–1052 (2016).
47. Allstate says losses from California fires $670M, CEO wants to address climate change. *Insurance Journal* (13 December 2018); https://go.nature.com/2GWG3K4
48. $8.6B worth of homes at high or extreme risk from California fires. *Insurance Journal* (16 November 2018); https://go.nature.com/3lnyCdK
49. Miller, R. E. & Blair, P. D. *Input-Output Analysis: Foundations and Extensions* 2nd edn (Cambridge Univ. Press, 2009).
50. Koks, E. E. & Thissen, M. A multiregional impact assessment model for disaster analysis. *Economic Syst. Res.* **28**, 429–449 (2016).
51. Mintz, D. *Technical Assistance Document for the Reporting of Daily Air Quality—the Air Quality Index (AQI)* (US Environmental Protection Agency, 2018).

Acknowledgements

We acknowledge the heroic efforts and sacrifices of the men and women who have fought California wildfires in recent years. This study was supported by the National Natural Science Foundation of China (41921005) and National Key R&D Program of China (2016YFA0602604). D.W. acknowledges support from the Fundamental Research Funds for the Central Universities (CXJJ-2020-301). D.G. acknowledges support from the National Natural Science Foundation of China (91846301 and 41629501), the UK Natural Environment Research Council (NE/N00714X/1 and NE/P019900/1), the Economic and Social Research Council (ES/L016028/1) and British Academy (NAFR2180103). S.S. acknowledges support from the National Natural Science Foundation of China (71922015 and 71773075). S.J.D. and M.M.K. acknowledge support from the US National Science Foundation and US Department of Agriculture (INFEWS grant EAR-1639318).

Author contributions

D.G. and S.J.D. designed the study. D.W., S.Z., G.G. and M.M.K. performed the analysis. D.G., S.J.D. and D.W. interpreted the results. D.W., S.J.D. and T.L. prepared the figures. D.W., S.J.D., D.G., S.Z. and G.G. prepared the manuscript. D.W., S.Z., G.G., T.L. and H.Z. prepared the supplementary information. D.G. coordinated and Q.Z., and P.G. supervised the project. Q.Z., S.S. and P.G. participated in the writing of the manuscript.

Competing interests

The authors declare no competing interests.

Additional information

Supplementary information is available for this paper at https://doi.org/10.1038/s41893-020-00646-7.

Correspondence and requests for materials should be addressed to D.G.

Peer review information *Nature Sustainability* thanks the anonymous reviewers for their contribution to the peer review of this work.

Reprints and permissions information is available at www.nature.com/reprints.

Publisher's note Springer Nature remains neutral with regard to jurisdictional claims in published maps and institutional affiliations.